

TO THE EDITOR:

G3BP2-KIT drives leukemia amenable to kinase inhibition in Ph-like ALL

Ilaria Iacobucci,^{1,*†} Reiji Fukano,^{1,*†} Jake D. Friske,¹ Chunxu Qu,¹ Laura J. Janke,¹ Yaqi Zhao,¹ Pradyumna Baviskar,¹ Emily A. Backhaus,¹ Peter Chockley,² Aman Seth,¹ A. Douglas Laird,³ Anjali S. Advani,⁴ and Charles G. Mullighan^{1,5,*}

¹Department of Pathology, and ²Department of Bone Marrow Transplantation and Cell Therapy, St. Jude Children's Research Hospital, Memphis, TN; ³Pfizer, Inc., La Jolla, CA;

⁴Cleveland Clinic, Cleveland, OH; and ⁵Hematological Malignancies Program, St. Jude Children's Research Hospital, Memphis, TN

Philadelphia-like (Ph-like) or *BCR-ABL1*-like B-cell precursor acute lymphoblastic leukemia (B-ALL) is genetically heterogeneous,^{1,2} with a gene expression profile similar to that of *BCR-ABL1*⁺ ALL.^{3,4} It comprises 15% to 30% of B-ALLs, with a peak of incidence in young adults.^{5,6} The most commonly mutated pathways are the ABL and JAK-STAT pathways with multiple rearrangements and lesions, which are druggable with a variety of tyrosine kinase inhibitors (TKIs).^{7,8} Rarer and more heterogeneous alterations, although often targetable with TKIs (eg, *ETV6-NTRK3*),⁹ may be missed by targeted genomic diagnostic approaches. We describe a case of Ph-like ALL and a novel gene fusion identified by RNA sequencing (RNA-seq) that juxtaposed exon 7 of *G3BP2* with exon 11 of *KIT* and encoded a fusion protein retaining the nuclear transport factor 2 domain of *G3BP2* and the entire kinase domain of *KIT*. In hematological malignancies, activating *KIT* mutations play a crucial role in systemic mastocytosis and acute myeloid leukemia¹⁰; however, fusions have not been described in leukemia or in other tumors.

We report a 52-year-old White man with second relapsed B-ALL after chemotherapy and blinatumomab (registered at www.clinicaltrials.gov as #NCT02013167).¹¹ A bone marrow aspirate specimen obtained at study entry in the INOVATE trial (#NCT01564784)¹² was analyzed by RNA-seq, given the patient's therapeutic resistance to date. At relapse, the patient had 51% blast cells in bone marrow by flow cytometric analysis. Of note, the patient was not treated with TKIs, and primary leukemia cells were not available for functional studies.

The fusion gene *G3BP2-KIT* was synthesized by the BioXp 3200 system (Codex DNA, Inc.) and cloned into a Gateway®-compatible c120–murine stem cell virus–internal ribosome entry site–green fluorescent protein (c120-MSCV-G3BP2-KIT-IRES-GFP) lentiviral vector. The truncated (TR) transcript portion of *KIT* fused to *G3BP2* and coding for amino acids 560 to 976 (TR KIT 560-976AA) was amplified and cloned (c120-MSCV-TR KIT 560-976AA-IRES-GFP). These constructs and the empty vector (MIG) were used for virus production and expression in interleukin-3 (IL-3)–dependent mouse hematopoietic Ba/F3 cells and IL-7–dependent ARF-null pre-B cells.¹³ Cell proliferation was examined in the absence and presence of cytokines. Sublethally irradiated (550 rad) 8-week-old wild-type C57BL/6 female mice underwent transplantation by tail vein injection of ARF-null pre-B cells expressing *G3BP2-KIT* or empty vector. Leukemia development was monitored by retroorbital bleeding; moribund mice were euthanized, and blood, bone marrow, and spleen samples were analyzed for evidence of leukemia by flow cytometry, histopathology, and genomic sequencing. Full methods are provided in the data supplement.

This B-ALL sample was predicted to be Ph-like B-ALL using prediction analysis of microarrays (Ph score, 1) and clustered with Ph-like B-ALL on t-distributed stochastic neighbor embedding analysis in our B-ALL subtyping pipeline.¹⁴ Moreover, RNA-seq detected a chimeric fusion between exon 7 of *G3BP2* (chromosome 4:76580296, hg19) and exon 11 of *KIT* (chromosome 4:55593611, hg19), juxtaposing the amino acid residues 2227 and 560 of *G3BP2* and *KIT*, respectively, and retaining the nuclear transport factor 2 domain of *G3BP2* and part of the catalytic domain and the entire kinase domain of *KIT* (Figure 1A; supplemental Table 1). This fusion was not previously detected in larger cohorts of B-ALL cases.^{2,5,14} Although

Submitted 27 April 2021; accepted 20 December 2021; prepublished online on *Blood Advances* First Edition 6 January 2022; final version published online 1 June 2022. DOI 10.1182/bloodadvances.2021004854.

*I.I. and R.F. contributed equally to this study.

†I.I. and R.F. are joint first authors.

RNA- and whole-exome sequencing data from mouse models have been deposited in the Sequence Read Archive under BioProject ID PRJNA717917. RNA-sequencing

data from the patient have been deposited in the European Genome-phenome Archive under EGAS00001005181.

The full-text version of this article contains a data supplement.

© 2022 by The American Society of Hematology. Licensed under Creative Commons Attribution-NonCommercial-NoDerivatives 4.0 International (CC BY-NC-ND 4.0), permitting only noncommercial, nonderivative use with attribution. All other rights reserved.

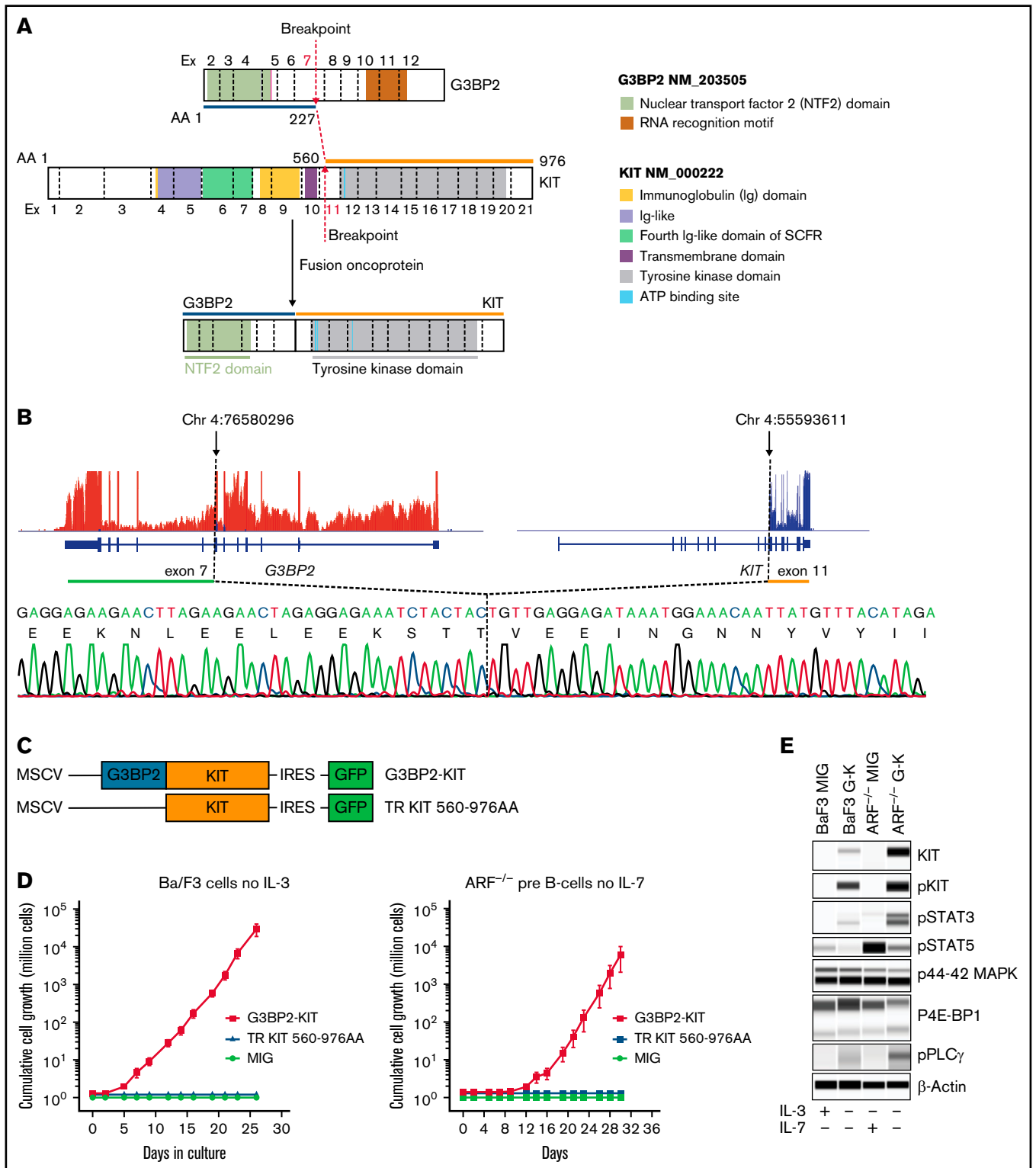


Figure 1. G3BP2-KIT fusion. (A) Schematic representation of wild-type G3BP2 and KIT and the chimeric fusion between exon (Ex) 7 of G3BP2 and exon 11 of KIT, juxtaposing the first 227 amino acids (AAs) of G3BP2 and the C-terminus portion of KIT including AAs 560 to 976. The joined Exs from both G3BP2 and KIT are in red and bold. The dotted red lines indicate breakpoint positions within Ex 7 and Ex 11 of G3BP2 and KIT, respectively. (B) Gene expression data for *G3BP2* and *KIT* from RNA-seq visualized by the Integrative Genomics Viewer showing overexpression of the *KIT* portion fused to *G3BP2* (hg19). Electropherogram shows the fusion junction between *G3BP2* and *KIT*. (C) Schematic representation of the viral vector used to express fusion protein G3BP2-KIT and TR KIT (TR KIT 560-976AA) in Ba/F3 cell lines and ARF-null pre-B cells. (D) Cytokine-independent assays in Ba/F3 cells and ARF-null pre-B cells expressing the chimeric transcript *G3BP2-KIT*, the only portion of *KIT* fused to *G3BP2* (encoding for AAs 560 to 976; TR KIT 560-976AA), or empty vector (MIG) cultured without recombinant mouse IL-3 or IL-7. (E) Whole-cell lysates from GFP⁺ sorted Ba/F3 and ARF-null pre-B cells were subjected to protein capillary electrophoresis with the Jess instrument (Protein Simple) with the following antibodies from Cell Signaling: KIT (#3074S), phosphorylated KIT (pKIT) Tyr719 (#3391S), pSTAT5 Tyr694 (#9359S), pSTAT3 Tyr705 (#9145S), pPLC γ 1 Tyr783 (#14008S), p44/42 MAPK (Erk1/2; #4695S), p4E-BP1 Thr37/46 (#2855S), and β -actin (#4970S). Borders are used for specifying different antibodies.

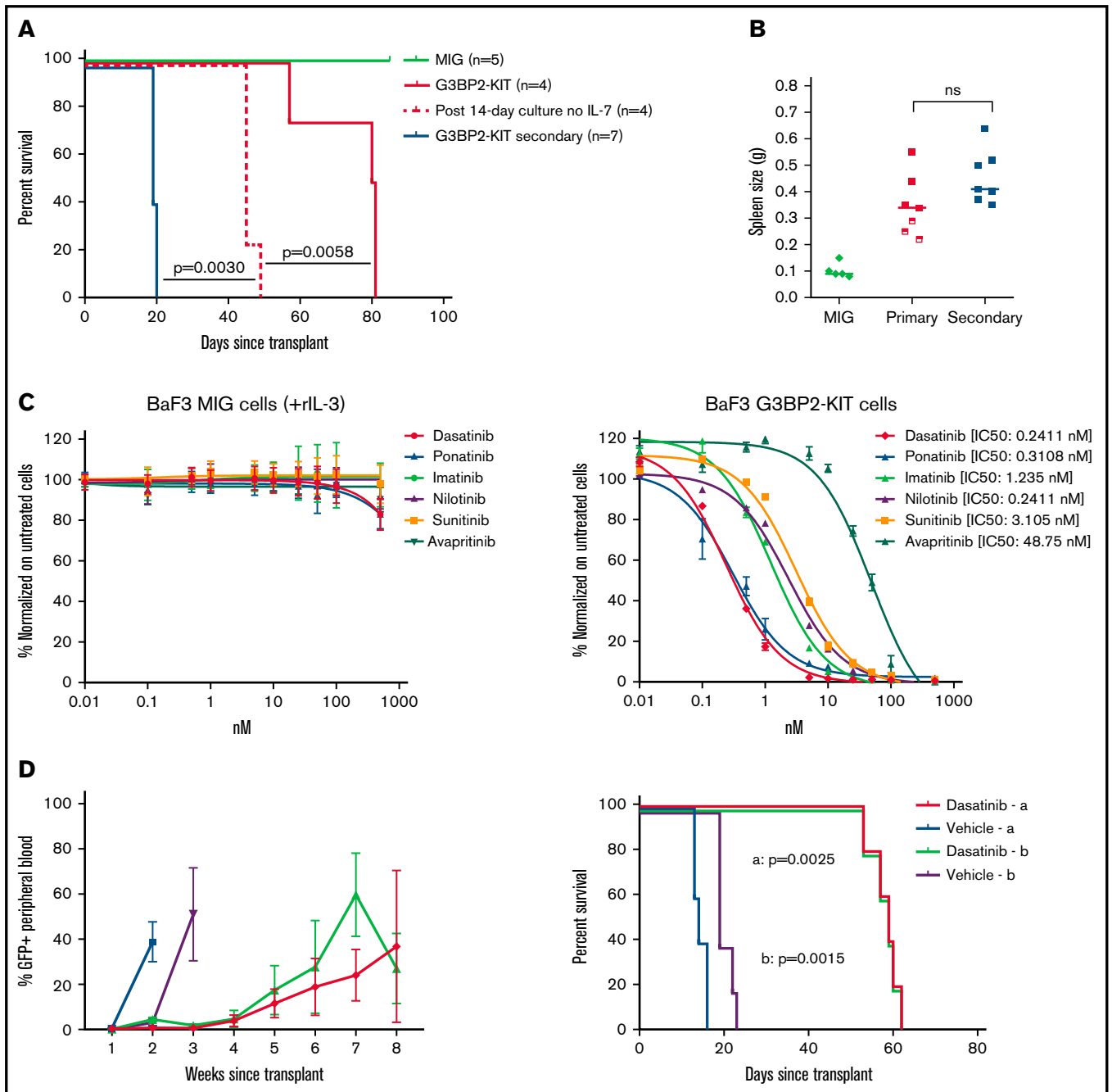


Figure 2. Genetically engineered mouse models of G3BP2-KIT leukemia. (A) Kaplan-Meier survival curves of C57BL/6 mice receiving ARF-null pre-B cell transplants expressing *G3BP2-KIT* (after 14 days in culture without IL-7 [$n = 4$] or within 48 hours after transduction [$n = 4$] or empty vector (MIG; $n = 5$) and of secondary recipients undergoing transplantation with cells from primary mouse tumors. Survival comparison was analyzed by log-rank test. (B) Spleen weight from primary and secondary recipient mice with *G3BP2-KIT* and from control mice (MIG). The mean weight is shown by the horizontal line in the scatter dot plot, and the error bars represent the standard deviations (SDs). (C) Dose-response curve of BaF3 cells expressing empty vector (MIG) or *G3BP2-KIT* fusion after 72 hours treatment with dasatinib, ponatinib, imatinib, nilotinib, sunitinib, or avapritinib. The cells transduced with the empty vector were grown in media with recombinant mouse IL-3. Values are normalized to dimethyl sulfoxide controls and represent means \pm SDs from 3 independent experiments performed in triplicate. (D) Left panel shows levels (means \pm SDs) of GFP⁺ cells in the peripheral blood of C57BL/6 mice receiving ARF-null pre-B leukemia cell transplants expressing *G3BP2-KIT* from 2 primary mouse tumor cohorts (a and b groups). In group a ($n = 5$), dasatinib (20 mg/kg daily) or vehicle ($n = 5$) was started 1 week after transplantation; in group b, treatment started 2 weeks after transplantation. Right panel shows Kaplan-Meier survival curves of mice in study treatment. IC₅₀, 50% inhibitory concentration; ns, not significant.

G3BP2 is ubiquitously expressed in the different hematopoietic lineages (supplemental Figure 1A), *KIT* is not normally expressed in B-lymphoid cells¹⁴ (supplemental Figure 1B). Thus, the fusion drives ectopic expression of the *KIT* transcript region fused to *G3BP2* in B cells, as demonstrated by RNA-seq (Figure 1B). Analysis of sequence mutations detected few additional alterations, but not in recurrently mutated genes in ALL, except for *ETV6*, *RPL22*, and *NT5C2*¹⁵ (supplemental Table 2), suggesting that the chimeric fusion transcript may have been a sufficient leukemogenic driver lesion in this patient. The fusion protein lacks the transmembrane domain of *KIT*, and immunofluorescence analysis of transiently transfected HEK293T cells showed a cytoplasmic localization (supplemental Figure 2A-B).

To investigate its oncogenic role, we cloned and expressed *G3BP2-KIT* fusion transcript, TR *KIT* (TR *KIT* 560-976AA), or empty viral vector in IL-3–dependent Ba/F3 (Figure 1C) and IL-7–dependent ARF-null pre-B cells (Figure 1D). Only the cells expressing *G3BP2-KIT* sustained cytokine-independent proliferation, suggesting that 5' *G3BP1* is necessary to confer oncogenic properties to TR *KIT*, likely by promoting *KIT* dimerization. Both Ba/F3 and ARF-null pre-B cells expressing *G3BP2-KIT*, but not those transduced with empty vector, showed phosphorylation of *KIT*, activation of JAK-STAT signaling with phosphorylated STAT3 and STAT5, MAPK pathway activation with phosphorylation of p44/p42 MAPK, and phosphorylation of phospholipase C (Figure 1E; supplemental Figure 3). Notably, transplantation of ARF-null pre-B cells expressing *G3BP2-KIT* in C57BL6 sublethally irradiated mice resulted in the development of serially transplantable B-ALL (Figure 2A), positive for B-cell lymphoid markers B220, CD19, and PAX5 (supplemental Figure 4A-B). Tumors were characterized by splenomegaly (Figure 2B) and multiorgan infiltration (supplemental Figure 4C). Whole-exome sequencing did not detect pathogenetic cooperating driver sequence mutations or copy-number changes (supplemental Table 3), confirming that *G3BP2-KIT* is a necessary and sufficient oncogenic driver alteration. Mouse leukemic cells showed enrichment of genes involved in JAK/STAT signaling (eg, *CSF3R*, *IL2RA*, *CXCL3*, *IL10RA*, and *PIK3R5*; supplemental Figure 4D-E), concordant with phosphorylation of STAT5 and STAT3 in Ba/F3 and ARF-null pre-B cells expressing *G3BP2-KIT* (Figure 1E).

Activating mutations in *KIT* have been described in acute myeloid leukemia, gastrointestinal stromal tumor, most cases of systemic mastocytosis, and other tumors.¹⁰ They result in activation of the receptor in the absence of ligand, playing a critical role in cell proliferation and differentiation. In these tumors where *KIT* deregulation is the driver oncogenic event, treatment with TKIs has been a successful approach.¹⁶ Therefore, we next examined the effect of kinase inhibition in Ba/F3 and ARF-null cell lines expressing *G3BP2-KIT*. These cells showed sensitivity to a wide range of TKIs with different specificities against *KIT* and the highest sensitivity to the dual SRC/ABL inhibitor dasatinib (Figure 2C; supplemental Figure 5A). In vitro treatment resulted in cell death and loss of *KIT* phosphorylation, indicating that constitutive activation of *KIT* is an important oncogenic signaling pathway for this fusion (supplemental Figure 5B). To confirm the efficacy of tyrosine kinase inhibition on leukemia cells in vivo, the established genetically engineered models of *G3BP2-KIT*–driven leukemia were randomized to receive dasatinib (20 mg/kg per day by oral gavage; n = 10) or vehicle (n = 10). Dasatinib prolonged survival in the engineered fusion mouse cell models, but it was not curative (Figure 2D).

G3BP2 is a member of the family of Ras-GTPase–activating SH3 domain–binding proteins, which includes 2 additional family members, *G3BP1* and *G3BP3*. These are RNA-binding proteins that are ubiquitously expressed and, under extracellular stresses, bind to untranslated regions of target transcripts and downregulate translation by either degrading the transcript or blocking ribosomal recruitment.¹⁷ Recently, a chimeric *G3BP1-PDGFRB* fusion sensitive to ABL1/PDGFRB kinase inhibition¹⁸ was described in a patient with a myeloid neoplasm with eosinophilia.

In conclusion, these results identify *KIT* rearrangement as a driver oncogenic alteration in leukemia and provide the rationale for therapeutic targeting with TKIs in *KIT*-rearranged Ph-like B-ALL.

Acknowledgments: The authors thank the Animal Resources Center and the Small Animal Imaging Center, the Compound Management Center, the Department of Chemical Biology & Therapeutics, the Department of Structural Biology for the use of BioXp 3200 system, the Genome Sequencing Facility of the Hartwell Center for Bioinformatics and Biotechnology, and the Flow Cytometry and Cell Sorting core facility of St. Jude Children's Research Hospital.

This work was supported in part by the American Lebanese Syrian Associated Charities of St. Jude Children's Research Hospital, the Leukemia and Lymphoma Society Translational Research Program (C.G.M.), a St. Baldrick's Foundation Robert J. Arceci Innovation Award (C.G.M.), the Henry Schueler 41 & 9 Foundation (C.G.M.), National Cancer Institute, National Institute of Health, Outstanding Investigator Award R35 CA197695 (C.G.M.), and a Research Agreement with Pfizer, Inc. (C.G.M.).

Contribution: I.I. designed, directed, and performed research, analyzed data, and wrote the manuscript; R.F., J.D.F., P.B., and E.B. performed research and analyzed data; C.Q. performed genomic analyses; L.J.J. performed histopathology analyses; Y.Z. performed sample processing; P.C. contributed to phosphoproteomic analysis; A.S. contributed to drug screening analysis; A.D.L. and A.S.A. contributed to conception and design of clinical sample analyses; C.G.M. edited the manuscript and gave final approval; and all authors critically reviewed the manuscript before submission.

Conflict-of-interest disclosure: I.I. reports honoraria from Amgen and Mission Bio. A.D.L. reports employment and stock and/or other ownership interests in Pfizer. A.S.A. reports consulting for Jazz Pharmaceuticals, Taiho Pharmaceutical, Team Pharmaceuticals, Amgen, Pfizer, Nkarta, Kite Pharmaceuticals, and Glycomimetics and research funding from Servier, Incyte, Amgen, Pfizer, Glycomimetics, Kite Pharmaceuticals, Seattle Genetics, Immunogen, and MacroGenics. C.G.M. reports research funding from AbbVie, Loxo Oncology, and Pfizer; speaking and travel fees from Illumina and Amgen; and stock ownership in Amgen. The remaining authors declare no competing financial interests.

ORCID profiles: I.I., 0000-0003-2008-1365; R.F., 0000-0002-4087-3426; J.F., 0000-0001-8987-8538; Y.Z., 0000-0002-8230-5312; E.B., 0000-0002-1253-9148; P.C., 0000-0002-5181-2696; A.S.A., 0000-0003-0015-5902; C.G.M., 0000-0002-1871-1850.

Correspondence: Ilaria Iacobucci, St. Jude Children's Research Hospital, 262 Danny Thomas Place, Mail Stop 343, Memphis TN 38105; e-mail: ilaria.iacobucci@stjude.org; and Charles G. Mullighan, St. Jude Children's Research Hospital, 262 Danny

Thomas Place, Mail Stop 342, Memphis TN 38105; e-mail: charles.mullighan@stjude.org.

References

1. Roberts KG, Morin RD, Zhang J, et al. Genetic alterations activating kinase and cytokine receptor signaling in high-risk acute lymphoblastic leukemia. *Cancer Cell*. 2012;22(2):153-166.
2. Roberts KG, Li Y, Payne-Turner D, et al. Targetable kinase-activating lesions in Ph-like acute lymphoblastic leukemia. *N Engl J Med*. 2014;371(11):1005-1015.
3. Den Boer ML, van Slegtenhorst M, De Menezes RX, et al. A subtype of childhood acute lymphoblastic leukaemia with poor treatment outcome: a genome-wide classification study. *Lancet Oncol*. 2009;10(2):125-134.
4. Mullighan CG, Su X, Zhang J, et al; Children's Oncology Group. Deletion of IKZF1 and prognosis in acute lymphoblastic leukemia. *N Engl J Med*. 2009;360(5):470-480.
5. Roberts KG, Gu Z, Payne-Turner D, et al. High frequency and poor outcome of Philadelphia chromosome-like acute lymphoblastic leukemia in adults. *J Clin Oncol*. 2017;35(4):394-401.
6. Tasian SK, Hurtz C, Wertheim GB, et al. High incidence of Philadelphia chromosome-like acute lymphoblastic leukemia in older adults with B-ALL. *Leukemia*. 2017;31(4):981-984.
7. Iacobucci I, Roberts KG. Genetic alterations and therapeutic targeting of Philadelphia-like acute lymphoblastic leukemia. *Genes (Basel)*. 2021;12(5):687.
8. Iacobucci I, Kimura S, Mullighan CG. Biologic and therapeutic implications of genomic alterations in acute lymphoblastic leukemia. *J Clin Med*. 2021;10(17):3792.
9. Roberts KG, Janke LJ, Zhao Y, et al. ETV6-NTRK3 induces aggressive acute lymphoblastic leukemia highly sensitive to selective TRK inhibition. *Blood*. 2018;132(8):861-865.
10. Abbaspour Babaei M, Kamalidehghan B, Saleem M, Huri HZ, Ahmadipour F. Receptor tyrosine kinase (c-Kit) inhibitors: a potential therapeutic target in cancer cells. *Drug Des Devel Ther*. 2016;10:2443-2459.
11. Dombret H, Topp MS, Schuh AC, et al. Blinatumomab versus chemotherapy in first salvage or in later salvage for B-cell precursor acute lymphoblastic leukemia. *Leuk Lymphoma*. 2019;60(9):2214-2222.
12. Kantarjian HM, DeAngelo DJ, Stelljes M, et al. Inotuzumab ozogamicin versus standard therapy for acute lymphoblastic leukemia. *N Engl J Med*. 2016;375(8):740-753.
13. Williams RT, Sherr CJ. The ARF tumor suppressor in acute leukemias: insights from mouse models of Bcr-Abl-induced acute lymphoblastic leukemia. *Adv Exp Med Biol*. 2007;604:107-114.
14. Gu Z, Churchman ML, Roberts KG, et al. PAX5-driven subtypes of B-progenitor acute lymphoblastic leukemia. *Nat Genet*. 2019;51(2):296-307.
15. Waanders E, Gu Z, Dobson SM, et al. Mutational landscape and patterns of clonal evolution in relapsed pediatric acute lymphoblastic leukemia. *Blood Cancer Discov*. 2020;1(1):96-111.
16. Roskoski R Jr. The role of small molecule Kit protein-tyrosine kinase inhibitors in the treatment of neoplastic disorders. *Pharmacol Res*. 2018;133:35-52.
17. Matsuki H, Takahashi M, Higuchi M, Makokha GN, Oie M, Fujii M. Both G3BP1 and G3BP2 contribute to stress granule formation. *Genes Cells*. 2013;18(2):135-146.
18. Jan M, Grinshpun DE, Villalba JA, et al. A cryptic imatinib-sensitive G3BP1-PDGFRB rearrangement in a myeloid neoplasm with eosinophilia. *Blood Adv*. 2020;4(3):445-448.